

Fourier and Wavelet Analysis for Optical Fibre Sensor Networks: A Review

Paul Childs, Xiujuan Yu, Allan C.L. Wong, Yan-Biao Liao, Gang-Ding Peng

Abstract—A review of the current state of research of Fourier analysis as applied to the field of optical fibre sensing is presented. The implications that using Fourier based multiplexing schemes have on the requirements for sensor design and network configuration is discussed. The flexibility of Fourier techniques is also demonstrated, with the ability to profile the fringe visibility or chirp of an interference spectrum. Generalisations of Fourier analysis to wavelet and chirplet analyses and their relevance to optical fibre sensor networks are also discussed.

Index Terms—Fourier transforms, harmonic analysis, multiplexing, optical fibre sensors.

I. INTRODUCTION

FOURIER analysis is a particular branch of the more general field of harmonic analysis, and is used to analyse the individual harmonic frequencies that exist in a given space by means of the Fourier transform [1] which breaks up the space into its individual constituent sinusoidal components with their relative phases intact (Herein only formulae for the continuous representations will be presented; the discrete versions being easily derived from them):

$$F(s) = \mathcal{F}(f(z)) = \int_{-\infty}^{\infty} f(z)e^{-2\pi izs} dz \quad (1)$$

The Fourier transform is traditionally used in optical sensing, as is the case for many conventional measurement technologies, for the interpretation of the, normally time varying, measured data. Periodic, or quasi-periodic, signals are isolated by the corresponding basis function (i.e. the exponential in the integrand) of eqn. (1); allowing an analysis of the constituent frequency components and their relative phases. Applications of this can be found in areas such as speech recognition using an acoustic sensor, determining gas concentrations with a chemical sensor and closed loop controlled system where tasks such as automatic alignment or damping of vibration is desired. This use of the Fourier transform as a standard signal processing tool is already well established forming the core material for many signal processing texts.

However, when the domain variable, z , represents wavelength or wavenumber, it can be seen that the Fourier transform can also be applied to the analysis of interferometric sensors, such

as Fabry-Perot [2], Sagnac [3], Mach-Zehnder [4]-[5] and Michelson interferometers [6], where the transmission and reflection spectrum is a periodic (and, in the case of all but that of the Fabry-Perot, sinusoidal) function of the wavenumber at zero dispersion. This paper presents a review of such a use of Fourier analysis for optical fibre sensors; extending further on the material previously presented in [7].

Fourier processing can either be performed electronically or optically. Digital signal processing has the benefits of greater flexibility, whereas, an all optical system has the benefit of processing at speed faster than can be possibly achieved using electronics. Nevertheless, the development of computational algorithms which reduce the number of operations from scaling as $O(N^2)$ to $O(N \log N)$ [8] and further numerical packages such as FFTW (Fastest Fourier Transform in the West) [9] as well as rapid advances made to computational processing speeds and the ability for these algorithms to be parallel processed (which reduces the time to $O(\log^2 N)$ [10] and the throughput to $O(\log N)$ [11]) allow for fast enough computation to satisfy the needs of most sensing applications.

The two basic measurements that can be made using Fourier analysis are spectral shifts and periodicity measurements. The dual Fourier relations governing this are:

$$f(z) \rightarrow f(z - \delta z) \Leftrightarrow F(s) \rightarrow F(s)e^{-2\pi i \delta z s} \quad (2)$$

$$\mathcal{F}(g(z)e^{2\pi i k z}) = G(s - k) \quad (3)$$

Assuming that $g(z)$ is a real valued function (thus $G(s)$ is hermitian and $|G(s)| = |G(-s)|$), the shift and period can be extracted from the respective phase and magnitude spectra of the Fourier domain as:

$$\delta z = \frac{d \arg(F)}{ds \ 2\pi} \quad (4)$$

$$k = \frac{\int s |G(s - k)| ds}{\int |G(s - k)| ds} \quad (5)$$

This method of measuring the shift and periodicity provides much more accurate measurements than conventional techniques that use peak detection, differentiation and zero crossing [12], etc. These conventional techniques have intrinsic

errors that cannot deal with situations where the peak is very flat, there is significant sidelobes around the peak, or when there is a skew effect due to the envelope of an interferometer [13]. The approach of eqn. (5), which exploits the symmetry in the Fourier domain, makes maximal usage of the available data; providing even greater accuracy than making use of the corresponding conventional techniques in the Fourier domain. Like all good wavelength based measurements, eqns. (4) and (5) are invariant of changes to the light source power (due to eqn. (4) being only dependent on the phase spectrum and eqn. (5) being self-referencing).

In recent years Fourier analysis has been increasingly used to improve the performance and multiplexing capabilities of grating based sensor networks [14]-[25]; devices that it is not so naturally suited to as was the case for interferometric sensors. This has come about in part by an increase in fundamental research into the inverse scattering problem that has assisted in the design of non-uniform grating structures. This has in turn enabled the production of fibre gratings with virtually arbitrary transmission spectra and group delay to meet the demands of advancing optical communications and sensing technologies. Although not all inverse scattering algorithms make use of Fourier analysis, the wider category of representation theory is common to all, and a complete overview of this field that is fundamental to understanding fibre grating technology will be looked at in section II. Section III, following it, will look at how Fourier techniques have enabled new and improved sensor multiplexing technologies and section IV will look at some further techniques to which Fourier analysis has recently been applied in optical fibre sensor systems.

As grating based sensors are not periodic, but rather have localised spectra, the use of Fourier analysis, which makes use of periodic non-localised basis functions $e^{2\pi is}$, is not necessarily the best approach. Wavelet transforms, which have localised basis functions, have been applied to the demodulation of fibre sensor signals [25]-[27]. An overview of the theory and techniques of wavelet transformation will be presented and further discussion as to its relevance to optical sensing will be given in section V.

II. SYNTHESIS AND RECONSTRUCTION

A. Inverse Problems in fibre grating devices

The response of a fibre optic sensor is dependent on the influence of the measurand at each point along its length and, for distributed sensing, it is often desirable to know how the measurand induced variations vary across the sensors length. This is the reconstruction problem, where e.g. a measured spectrum is used to determine the structure of a sensor. A similar problem is the synthesis problem, where a desired

spectrum is used to determine what the structure of the sensor needs to be in order to achieve it. These inverse problems are traditionally carried out using the approach of Gel'fand, Levitan and Marchenko (GLM) [28]-[29], who used integral equations to determine the form of a differential equation (DE) based on its boundary conditions:

$$f(x, y) + \int_0^x f(y, t)K(x, t)dt + K(x, y) = 0 \quad (6)$$

where f is a Fourier function determined by the boundary conditions of the DE (the scattering data) and K is an integration kernel used in expressing the Jost solution of the DE in terms of travelling waves (from which the scattering potential can be determined). Using such an approach yields a solution; however, performing the numerical integration is computationally demanding and ideally requires some form of optimisation to speed up the process.

The coupled mode equations:

$$\begin{aligned} \partial_z A &= ikA + q * B \\ \partial_z B &= -ikB \pm qA \end{aligned} \quad (7)$$

can arise in the solution of the Cauchy problem of the cubic Schrödinger equation [30], which has led to their description as the "Zakharov-Shabat system" (ZS) in the context of inverse scattering. In this case, inverse scattering attempts to find the function q from a knowledge of the boundary conditions of A and B . Expressing eqn. (7) as a matrix equation, and making the required modifications to eqn. (6) to put it in a coupled vectorial form gives for the counter-propagating (+ q) case:

$$\begin{aligned} 0 &= f(z+x) \begin{pmatrix} 0 \\ 1 \end{pmatrix} + \begin{pmatrix} K_1(z, x) \\ K_2(z, x) \end{pmatrix} \\ &+ \int_{-\infty}^z f(x+t) \begin{pmatrix} K_2^*(z, t) \\ K_1^*(z, t) \end{pmatrix} dt, \quad x < z \end{aligned} \quad (8)$$

$f(x, y)$ in this context is the Fourier transform of the complex reflection coefficient (plus integration around zeros in the appropriate complex half plane) and is only necessarily of one variable, $x+y$. The coupling coefficient $q(z)$ can be found from the lower term of the integration kernel as [30]:

$$q(z) = 2 \lim_{t \rightarrow z} K_2(z, t) \quad (9)$$

The GLM-ZS approach can be greatly improved in terms of computational speed by making use of the inherent causality that occurs within the ZS system. Let us discretise the optical device into several "layers" where q is piecewise constant (the so called Goupillaud medium). The GLM equations make use of Hardy spaces, i.e. the response of a medium must be quiescent (have zero signal) before an initial impulse at $t=0$. Due to this, the initial response for the counter-propagating case at $t=0$ must be entirely due to the first layer of the device and the initial response for the co-propagating case at time $t=N\tau_f$ must be due to propagation along the fast mode only (N layers of time τ_f). For the case in reflection, iteration continues

one layer at a time (as is shown in fig. 1); the coupling constants of previously evaluated layers determining the truncated impulse response, the mismatch of which with the measured impulse response in turn determines the coupling constant of the new layer. For the case in transmission things are more complicated due to all the layers being interrelated.

This approach is known as a layer peeling algorithm. It was devised by geophysicists Robinson [31] and Goupillaud [32] who applied it to the determination of seismic structure. Several different layer peeling methods have been developed for the ZS system for the case of Fibre Bragg Gratings (FBGs) [33]-[36] and Long Period Gratings (LPGs) [37]. When properly optimised, the number of computational operations for these algorithms scales as $O(N^2)$. These methods are known as the time-frequency domain layer peeling (TFDLP) method ([33] with enhancements given in [38]), the frequency domain layer peeling (FDLP) method [34], the time domain layer peeling (TDLP) method [35] and the integral layer peeling (ILP) method [36]. The latter of these is actually a hybrid method between taking the approach of layer peeling and performing the numerical integration of the GLM equations. Another recent approach, known as the Toeplitz inner-bordering (TIB) method ([39] with enhancements given in [40]), solves the GLM equations, but makes use of the inherent Toeplitz symmetry of the matrix equations involved in order to achieve the required $O(N^2)$ number of operations for fast processing.

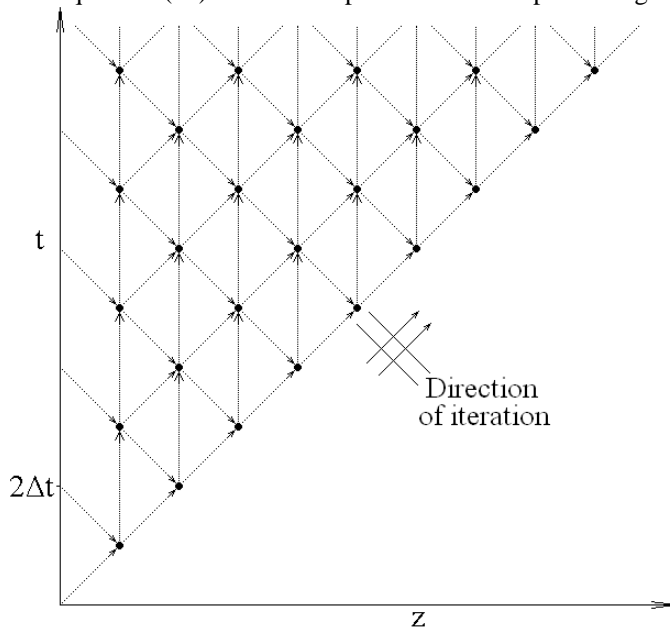


Fig. 1. Schematic of a layer peeling process for the counter-propagating case, where scattering events are represented as a discrete lattice of dots in space and time (Δt is the propagation time between layers). Arrows pointing diagonally up and to the right indicate the forward propagation in time, and building up of, the truncated impulse response, Arrows pointing diagonally down and to the right indicate the back propagation of the actual impulse response. Where these intersect at a lattice point, the coupling constant (and those of all lattice points vertically above as it doesn't change with time - arrows pointing up) can be determined provided the arrows have propagated along a path of lattice points

of known coupling constants. Iteration thus continues scanning up and to the right.

Apart from being inherently part of the structure of the GLM equations (in the theory of Hardy spaces and determining the function f), Fourier analysis plays a strong role for the case of algorithms that exhibit a time-frequency domain, or just a pure frequency domain, approach. The impulse response and the reflection spectrum are related by a Fourier transform linking the frequency domain expression of the reflectivities of the layers already determined to the time domain expression of the reflectivity of the layers up to the one yet to be determined. This is equivalent to the zeroing in process in t and z of the limit in eqn. (9).

Errors involved in layer peeling come from the errors involved in processing each layer and generally accumulate exponentially [35],[41]. A comparison of the FDLP, TFDLP and TDLP methods tested in [42] shows that the amount of error accumulation is much less for the case of time domain methods indicating that the majority of this error comes from trigonometric calculations involved in the FFT. As a result it is expected that frequency domain methods will be phased out of use as numerical algorithms, though they will still likely remain of use for understanding the process of inverse scattering. The TIB method is still relatively untested, but due to the inherent numerical stability and lack of simplifying assumptions made could be expected to replace the layer peeling methods entirely.

B. Reconstruction: Finding the location of a measurand

Reconstruction plays a role in sensing in that it allows one to determine the spatial variation of the measurand(s), giving more of a measure of distributed sensing rather than just treating the fibre sensors as point sensors. Due to having less reconstruction error [35], as well as being more readily able to apply simplifying assumptions, chirped gratings (where the resonant wavelength varies across the length of the grating) are most often employed in these situations. Such assumptions are often needed in order to achieve real time processing by reducing the computational time down from an order $O(N^2)$ process to one of order $O(N)$ and/or increasing the data collection rate of the swept wavelength system by eliminating the need for phase measurements (e.g. [43],[44]). Applications where reconstruction has played a role in determining the spatial variation of a measurand include distributed strain and temperature sensing [45], crack monitoring in concrete and composite structures [46], fatigue and wear monitoring in industrial process control [47], as well as characterising the photosensitivity of fibres used in fabricating the FBG sensors [48]-[49].

For the case of grating synthesis, the uniqueness of the solution is not a problem, because any solution will suffice. However, for the case of reconstruction, if there are multiple (or an

infinite number of) inverse solutions to a given set of scattered data then one can potentially be grossly mistaken by determining the measurand based on one of these. This is more of a problem for LPGs than for FBGs as FBGs only require the complex reflection spectrum in order to uniquely reconstructed them (the complex transmission spectrum can be derived due to conservation of energy and causality [50]), whereas LPGs require both the complex core-to-core and core-to-cladding transmission coefficients (the latter of which is very difficult to obtain experimentally). It has been shown, though, that by altering the system architecture a reconstruction can be performed using only a complex core-to-core transmission spectrum measurement [51].

III. MULTIPLEXING

The Fourier series forms an orthogonal basis on the measured data set. A component of the Fourier spectrum that is unique to one sensor will allow that sensor to be monitored using orthogonal detection, in the idealised sense without crosstalk from any other sensors that occupy the same wavelength or time channel [52]. The Fourier domain can thus be divided up like the wavelength domain is for Wavelength Division Multiplexing (WDM); an example of which is shown in fig. 2.

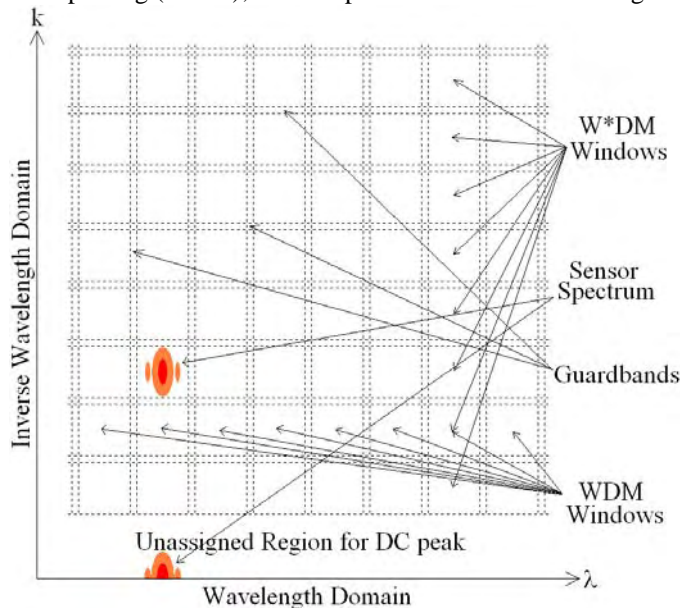


Fig. 2. Domain division access for multiplexing in the wavelength domain and its Fourier dual domain.

In order to fit within the grid of a multiplexing model, such as the type shown in fig. 2, the sensor will not only be constrained in terms of wavelength and bandwidth, but also in terms of a certain type of spectral shape due to limitations in the Fourier domain. The transmission spectrum of a FBG that satisfies the

requirements to be multiplexed and demultiplexed using Fourier decomposition is given by [15] as:

$$T^{(j)} = 10^{-\frac{L}{10} \left[\cos^2 \left(\frac{(j+\eta)\pi\delta\lambda}{d} \right) \text{sinc}^2 \left(\frac{(1-\zeta)\delta\lambda}{2d} \right) \right]} \quad (10)$$

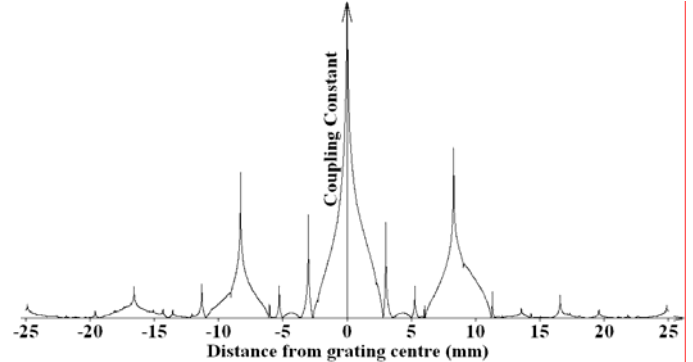


Fig. 3. Grating profile for $j=1$.

where j is the channel number that the grating will appear in the Fourier domain, $\delta\lambda$ is the detuning from the resonant wavelength, L is the transmission dip depth of the FBG, d is a parameter related to the sampling resolution and the maximum channel capacity and η and ζ are variables governing the guardband widths. Applying a layer peeling algorithm [38] to this gives the spatial variation of the index perturbation as is shown in fig. 3 for the case of $j=1$. It should be noted that fabrication constraints will cause a deviation from this idealised structure. Furthermore, differential measurand variations can have a large effect on the stability of the spectrum [53], though for certain applications this may prove to be useful.

The Fourier transform operates on linear vector spaces and as such requires the spectrum (which is a product of the SU(2) transmission matrices) to be linearised first. The best to which this can be achieved is by making a scalar approximation (which ignores multiple scattering) and conjugating as [15]:

$$X : D\{R^{(j)}\} \rightarrow \log_2 D\{2^{R^{(j)}}\} \quad (11)$$

The spectrum can then be transformed and analysed. Modifying eqn. (4), the change in wavelength can be determined as [15]:

$$\delta\lambda = \frac{\Delta\lambda}{2\pi} \left\langle \frac{d}{ds} \tan^{-1} \left(\frac{\text{Im}(\mathcal{F}(X))}{\text{Re}(\mathcal{F}(X))} \right) \right\rangle \quad (12)$$

where $\Delta\lambda$ is the width of the WDM channel, the \tan^{-1} function includes phase unwrapping and the expectation value brackets " $\langle \dots \rangle$ " denote a suitable weighted average over the peak in the magnitude spectrum of the Fourier domain corresponding to the grating (this method of weighting gives less error than say a linear regression [54] which is more sensitive to the end points where the phase error is greater due to the reduced level of the magnitude spectrum). The accuracy of eqn. (12) is only dependent on the grating bandwidth and as such is superior to other techniques such as peak detection and zero crossing, etc.,

where flat regions of the grating spectrum or skew effects [13] may cause errors.

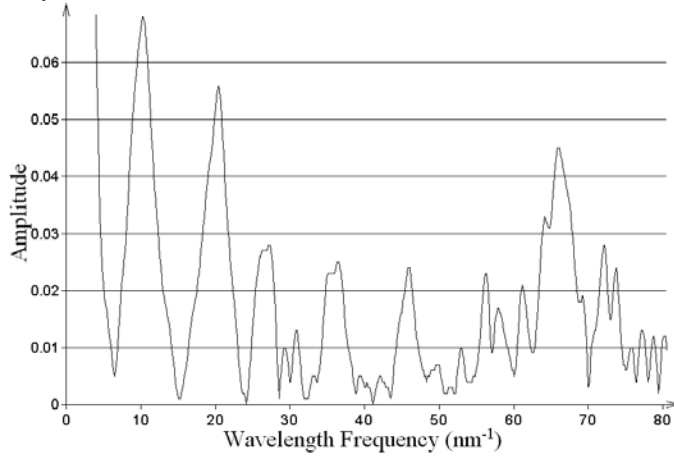


Fig. 4. Peaks in the Fourier domain allowing the identification of 8 sensors multiplexed with the same nominal Bragg wavelength (The peak of the seventh sensor isn't depleted as much as neighboring peaks as its Bragg wavelength is perturbed by the measurand so that it only partially overlaps the bandwidth of the other sensors) [17]

For the case where eqn. (11) is not applied, 5 weakly reflecting narrowband gratings [20] and 50 weakly reflecting gratings occupying the entire C band (thus being incompatible with WDM) [21] have been multiplexed using a Fourier based multiplexing. With eqn. (11) applied, 8 strongly reflecting gratings with more localised spectra have been multiplexed (see fig. 4) [17], but with the potential to easily extend to a total network of 64 sensors using WDM. As such, large sensor counts suitable for applications such as monitoring large scale structures can be achieved. This degree of multiplexing brings down the cost per unit sensor such that optical sensing is able to compete with conventional sensing technologies as an economically viable technology.

Crosstalk occurs between sensors when there is a mixing of the signal between two sensors that is not properly separated during demultiplexing. This can come about from two causes. Firstly, the fabrication of the grating may be non-ideal; with a sensor having a Fourier spectrum that overlaps a component (or range of components) of the Fourier spectrum that is used for detection of another sensor. Secondly, nonlinearities caused by the sensor network architecture can cause frequency components of one or more sensors to mix giving a frequency that corresponds to another sensor [55].

In both cases crosstalk generally occurs from a sensor with lower Fourier frequencies to sensors of higher Fourier frequencies [16], in the former case as non-ideal fabrication generally causes higher harmonics in the Fourier domain to appear, and in the latter case as the nonlinear mixing of sensors favours higher frequency generation [55]. In the former case the crosstalk is significantly less than what a simplistic

quantitative analysis obtained from performing a relative measurement of the overlap integral of the Fourier spectrum of the two sensors would suggest [56]. Further research into this is ongoing. For the latter case, a statistical study of the crosstalk error for various sensor network sizes and sensor reflectivities has been performed and is presented in fig. 5. To achieve error levels below a moderate value of $10\mu\epsilon$ on a realistic system, it is shown that it is impossible to extend the sensor network capacity beyond 20 sensors.

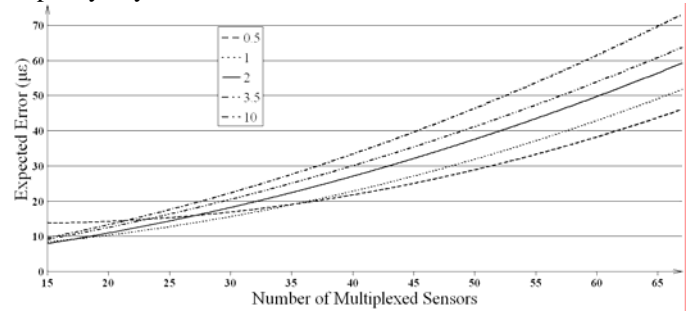


Fig. 5. Expected Crosstalk Error for various FBG sensor network sizes and sensor reflectivities (legend in dBs) [55].

IV. OTHER USES

Fourier transformation is not just useful for determining the movement of sinusoidal components in a given spectrum; it can also be used to extract information based on changes in the nature of those components. Sinusoidal signals can be amplitude or phase modulated and both changes to the amplitude as well as nonlinear changes to the phase can both be extracted from a signal using Fourier analysis.

A. Visibility of Fringes

A number of evanescent sensors make use of gratings with in-line Michelson, Mach-Zehnder or ring structures [57]-[59], with one mode propagating as the guided core mode and the other as one of the cladding modes. Losses to the cladding mode leave less power to cause interference and thus reduce the visibility of fringes.

As:

$$1 + v \cos(2\pi k \lambda) \rightarrow \delta(s) + \frac{v}{2} [\delta(s - k) + \delta(s + k)] \quad (13)$$

the visibility can thus be reconstructed from the magnitude spectrum of the Fourier domain as twice the area of either the positive or negative frequency peak corresponding to the interference divided by the area of the zero frequency peak:

$$v = \frac{\langle |G(s \mp k)| \rangle}{\langle |G(s)| \rangle} \quad (14)$$

The area is used as the visibility of fringes will generally vary across a spectrum, in which case the value of v on the RHS of eqn. (13) is different to that of the LHS (related by Fourier

transformation) and acts by convolution rather than multiplication. As the visibility is expected to vary slowly with the spectrum, its dual representation on the RHS should be localised enough that there will be no overlap with the zero frequency delta function and the area thus provides an effective mean of the visibility spectrum.

This provides a very stable mechanism for determining measurand changes as it inherently has both amplitude and phase invariance. The measured sensor spectrum consists of an envelope amplitude spectrum multiplied by the interference term; i.e. the LHS of eqn. (13). In the dual domain the transform of this envelope spectrum (and variations thereof) acts on the RHS of eqn. (13) by convolution. Provided the transform is sufficiently compact that the broadening does not cause the zero frequency and interference peaks to overlap, the two peaks can still be distinctly identified. As convolution is area preserving, the division of areas of the peaks in eqn. (14) is invariant to the amplitude spectrum and thus to any instabilities in the light source.

The phase invariance of the visibility of fringes measurement comes about as a result of only requiring the magnitude spectrum, which in eqn. (2) is unchanged. There is even greater phase stability in that, although the value of k is needed to locate the window over which to determine the area of the interference peak, if the peak is confined well enough within this window then small changes in k are also not going to affect the visibility measurement. The visibility measurement is thus stable against any spectral shifts, which is a particular issue when using LPGs or other devices with a high degree of cross sensitivity.

There is, however, a deterioration of the measured value of the visibility of fringes if chirp is introduced into eqn. (13). Spectrally, nonlinearities in the argument of the cosine interference can be examined by expanding them as a Fourier series of terms that apply frequency modulation to the base frequency k , which in turn expand by the Jacobi-Anger expression as a series of Bessel valued sidebands. This process of splitting into all these terms does not in general preserve area (by Parseval's theorem it is the square of the magnitude that is conserved), and as a result it may be better to opt for a root mean square approach for the expectation values of eqn. (14) in cases where there may be a significant amount of chirp present. Alternatively, the chirp can be quantitatively analysed (as listed below) and used to compensate for the depletion of the measurement of the visibility of fringes.

An example application of visibility of fringes measurements is shown in fig. 6, where the humidity can be monitored from a pair of LPGs (arranged as a Mach-Zehnder interferometer) with a hydrogel coating between them which alters the cladding

mode. It has been shown for this sensor that measurements based on the visibility of fringes provide a much greater linearity and repeatability than measurements based on the wavelength shift [60].

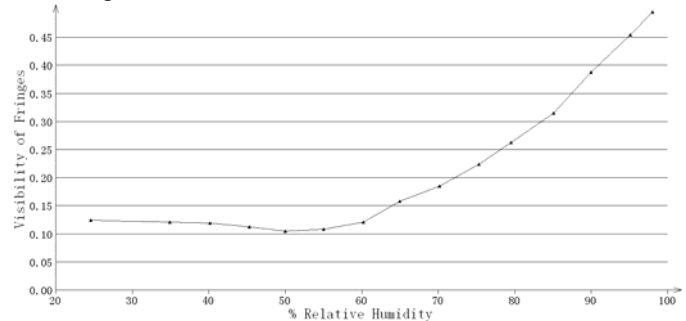


Fig. 6. Change in fringe visibility for a cascaded LPG based humidity sensor.

Similarly, visibility of fringes measurements have been used to accurately measure the external refractive index from a pair of blazed FBGs (arranged as a mono-directional ring cavity) [59].

As such it can be seen that visibility measurements using Fourier techniques form a greatly useful and highly stable method to demodulate signals, particularly from evanescent fibre sensors.

B. Chirp and Dispersion

Chirp, which appears as a nonlinear dependence of the phase of a sinusoidal interference upon wavelength can also be measured by developing inverse solutions such as eqn. (4), but based on the Fourier relations:

$$\mathcal{F}\left(e^{ik_2\lambda^2}\right)\{s\} = \sqrt{\frac{\pi}{k_2}} e^{-i\left(\frac{\pi^2 s^2}{k_2} - \frac{\pi}{4}\right)} \quad (15)$$

$$\mathcal{F}\left(e^{ik_3\lambda^3}\right)\{s\} = \frac{2\pi}{\sqrt[3]{3k_3}} \text{Ai}\left(\frac{-2\pi s}{\sqrt[3]{3k_3}}\right) \quad (16)$$

where eqn. (15) shows the transform of a linear chirp (with phase quadratic in wavelength) and eqn. (16) that of a quadratic chirp (with phase cubic in wavelength). The RHS of eqn. (15) can easily be solved for k_2 , whereas that of eqn. (16) requires a numerical approach to determine k_3 .

Chirp can be caused by various forms of dispersion in the fibre or due to time lag effects within the component that provides the splitting and recombination of the interference. Even where there is no dispersive effect, chirp will be seen in an interferogram for the case where the measurand is changing during the period of time it takes to scan over the wavelength range. Thus a measurement of chirp can be used as a means to determine what effect a measurand has upon the dispersion in a

fibre, or as a self-evaluating test of the quality of experimental control exercised.

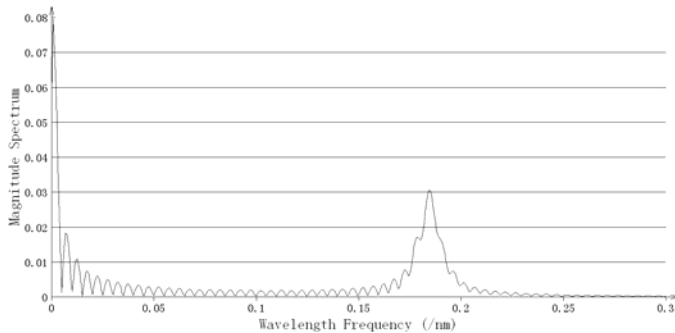


Fig. 7. Fourier spectrum of a Sagnac interferometer made from highly birefringent photonic crystal fibre showing significant broadening due to linear chirp and partial asymmetry due to quadratic chirp.

An example of a Fourier spectrum of an interferometer with a high degree of nonlinearity (a Sagnac interferometer using highly birefringent photonic crystal fibre) is shown in fig. 7. The presence of such higher order nonlinearities creates a broadening of the peaks measured in the Fourier domain (with the exception of the zero frequency peak, whose width only depends on the envelope spectrum). The asymmetric odd order terms will also shift the apparent location of the peak, whether this is visually determined or evaluated using eqn (5). Performing an analysis of the higher order terms allows for a more accurate depiction of the interferometric effects in the sensors and ultimately an improved analysis of the measurand(s).

V. WAVELET ANALYSIS

Where Fourier analysis is part of a wider field known as harmonic analysis, which allows analysis to be performed on more generalised spaces than L^2 (i.e. the space spanning the square integrable functions) used by Fourier analysis, harmonic analysis is part of a wider field known as representation theory where the restrictions are looser and allow for a wider variety of tools. Instead of projecting onto the space spanned by $e^{2\pi is}$ (each component of which is infinitely spread out in time unlike any realistic signals), wavelet transforms project to a family of functions given by dilations and translations of coherent states (the wavelet) that have a measure of localisation in both time and frequency [61].

The wavelet transform grew out of studies of the affine group [62] and engineering developments in designing quadrature mirror filter banks [63]. The main goal of these developments was to design filter banks that would allow signals to be multiplexed and demultiplexed without any alteration of the signal as a result of this process. For this to happen, certain

conditions need to be met by the filter banks [64]. The wavelets that correspond to filter banks in general form non-orthogonal basis sets (with a few exceptions, such as the Daubechies wavelets), which means that the reconstruction is not necessarily unique and thus the reconstructed signal may be different from the original signal.

One of the intrinsic properties about wavelet based reconstructions is their multi-resolution capability [65]-[66]. Wavelets corresponding to higher frequencies are obtained by dilation to a smaller size, which also gives them the ability to resolve at a finer scale in the time domain. This is generally more useful for applications such as speech and other forms of acoustics, where the varying resolution scale corresponds more realistically to the way in which the human ear perceives sound. However, it is also a useful property for the transmission and analysis of signals in general.

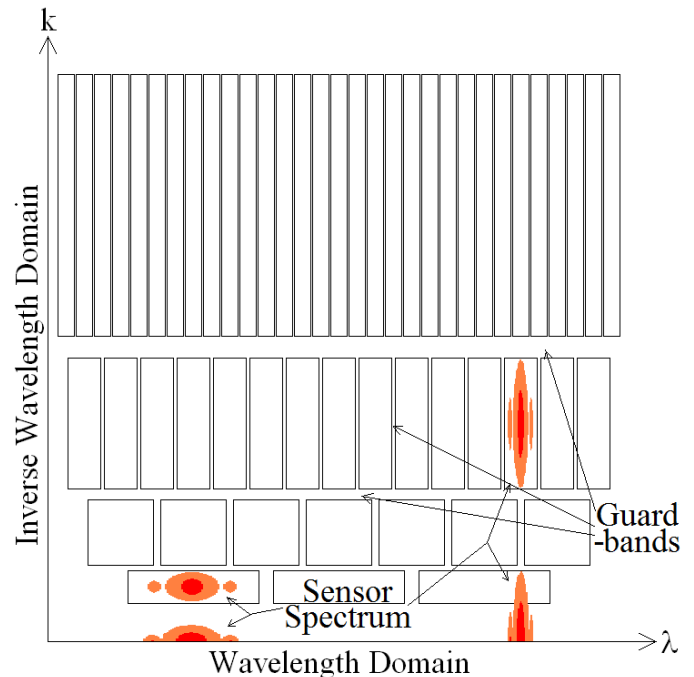


Fig. 8. Multiresolution domain division access for multiplexing in the wavelength domain and a dual domain based on wavelet decomposition.

An application of the multiresolution capability of wavelets (in this case in the form of a binary tree decomposition) to multiplexing would alter the domain representation from that given in fig. 2 to what is shown in fig. 8. The measurement range and accuracy can be seen to vary between the different vertical wavelet levels. In the higher levels there is not much space in the wavelength for the sensors to operate over, but there are a lot of data points in the inverse domain to accurately determine any shifts. The contrary is the case for lower levels.

Tailoring of the distribution and shape of the wavelet windows is also possible by controlling the scaling of the wavelets. This gives a multiplexed sensor network based on wavelet decomposition the flexibility to tailor the performance of individual sensors in the network to match the various measurement needs associated with the given application that can vary from point to point and with different measurands. One thing to note, though, is that there are also heavier restrictions on the amount of useable spectral space due to potential overlaps of the generally wide-in-inverse-wavelength DC peaks of high level sensors with windows of lower level sensors. For the case of sensors with a large amount of chirp in their interference spectrum mentioned above (and particularly sensors having increasing chirp with inverse wavelength) the DC peak is proportionally much narrower (see fig. 7) and such a distribution would make an ideal fit.

Further generalisations of the wavelet transform have also been made, e.g. the chirplet transform [67], where the family of functions is extended to allow variations in chirp along with the existing translation and dilation operations of the mother wavelet. This can be used for tailoring of the wavelet windows of fig. 8 to tilt off axis (as can be done with the fractional Fourier transform to that of fig. 2) as well as providing a more natural basis for analysing chirped signals. Wavelet and chirplet approaches, for instance, allow one to more naturally perform intra-grating sensing on chirped gratings; monitoring changes in the measurand(s) along the length of the fibre.

VI. CONCLUSION

A review of Fourier theory applied to the field fibre optic sensing was presented. Areas of multiplexing, grating design and various spectral analyses were covered.

REFERENCES

- [1] J.B.J. Fourier "Mémoire sur la propagation de la chaleur dans les corps solides (extrait)" in *Nouv. Bull. Sci. Soc. Phil. Paris*, T. 1, No. 6, pp. 112-116, 1808 (in French).
- [2] S.M. Musa "Real-time signal processing and hardware development for a wavelength modulated optical fiber sensor system" Ph.D. Dissertation, Virginia Polytechnic Institute and State University, 1997.
- [3] G. Sagnac "Strioscopie et striographie interférentielles analogues à la méthode optique des stries de Foucault et de Töpler" in *Compt. Rend. Acad. Sci. Paris*, T. 153, No. 2, pp. 90-93, 1911 (in French).
- [4] L. Zehnder "Ein neuer interferenzrefraktor" *Z. Instrkde*, T. 11, h. 8, s. 275-285, 1891 (in German).
- [5] L. Mach "Über einen interferenzrefraktor" *Z. Instrkde*, T. 12, h. 3, s. 89-93, 1892 (in German).
- [6] A.A. Michelson, and E.W. Morey "On the relative motion of the earth and the luminiferous aether" in *Phil. Mag.* S. 5, Vol.24, No. 151, pp.449-463 (1887).
- [7] P.Childs, X.J. Yu, A.C.L. Wong, Y.B. Liao and G.D. Peng "Fourier analysis for optical fibre sensor networks" in *Proc. ISMOT*, New Delhi, India, 16-19 Dec (2009)
- [8] J.W. Cooley, and J.W. Tukey "An algorithm for the machine calculation of complex Fourier series" in *Math. Comp.*, Vol. 19, No. 90, pp. 297-301 (1965).
- [9] M. Frigo, and S.G. Johnson "The design and implementation of FFTW3" in *Proc. IEEE*, Vol. 93, No. 2, pp. 216-231 (2005).
- [10] M.C. Pease "An adaptation of the fast Fourier transform for parallel processing" in *J. ACM*, Vol. 15, No. 2, pp. 252-264 (1968).
- [11] C.D. Thompson "Fourier transforms in VLSI" in *IEEE Trans. Comp.*, Vol. C-32, No. 11, pp. 1047-1057 (1983).
- [12] A.D. Kersey, T.A. Berkoff, and W.W. Morey "Multiplexed fiber Bragg grating strain-sensor system with a fiber Fabry-Perot wavelength filter" in *Opt. Lett.*, Vol. 18, No. 16, pp. 1370-1372 (1993).
- [13] B.H. Lee, and J. Nishii "Dependence of fringe spacing on the grating separation in a long-period fiber grating pair" in *Appl. Opt.*, Vol. 38, No. 16, pp. 3450-3459 (1999).
- [14] M.G. Shlyagin, S.V. Miridonov, D. Tentori, F.J. Mendieta, and V.V. Spirin "Multiplexing of grating-based fiber sensors using broadband spectral coding" in *Proc. SPIE*, Vol. 3541, pp. 271-278 (1999).
- [15] P.Childs "An FBG sensing system utilizing both WDM and a novel harmonic division scheme" in *J. Lightw. Technol.*, Vol. 23, No. 1, pp. 348-354 (2005); "Erratum" Vol. 23, No. 2, pp. 931 (2005).
- [16] P. Childs, A.C.L. Wong, and G.D. Peng "A Strain Sensor System Based on Carrier Modulated Gratings for the Monitoring of a Large Number of Channels" in *J. Lightw. Technol.*, Vol. 24, No. 3, pp. 1388-1394, (2006).
- [17] P. Childs, and G.D. Peng "Simultaneous detection of 8 spectrally overlapping carrier modulated Fibre Bragg Gratings" in *Electron. Lett.*, Vol. 42, No. 5, pp. 274-275 (2006).
- [18] Y.J. Rao, Z.L. Ran, and C.X. Zhou "Fiber-optic Fabry-Perot sensors based on a combination of spatial-frequency division multiplexing and wavelength division multiplexing formed by chirped fiber Bragg grating pairs" in *Appl. Opt.*, Vol. 45, No. 23, pp. 5815-5818 (2006).
- [19] R.P. Murphy, S.W. James, and R.P. Tatum "Multiplexing of fiber-optic long-period grating-based interferometric sensors" in *J. Lightwave Technol.*, Vol. 25, No. 3, pp. 825-829 (2007).
- [20] M.G. Shlyagin, S.V. Miridonov, D. Tentori, F.J. Mendieta, and V.V. Spirin "Multiplexing of grating-based fiber sensors using broadband spectral coding" in *Proc. SPIE*, Vol. 3541, pp. 271-278 (1998).
- [21] Z. Wang, F. Shem, L. Song, X. Wang, and A. Wang "Multiplexed fiber Fabry-Pérot interferometer sensors based on ultrashort Bragg gratings" in *IEEE Photon. Technol. Lett.*, Vol. 19, No. 8, pp. 622-624 (2007).
- [22] A.C.L. Wong, P.A. Childs, and G.D. Peng "Multiplexing technique using amplitude-modulated chirped fiber Bragg gratings" in *Opt. Lett.*, Vol. 32, No. 13, pp. 1887-1889 (2007).
- [23] M. Jiang, Z.G. Guan, and S. He "Multiplexing scheme for self-interfering long-period fiber gratings using a low-coherence reflectometry" in *IEEE Sensors J.*, Vol. 7, No. 12, pp. 1663-1667 (2007).
- [24] A.C.L. Wong, P.A. Childs, and G.D. Peng "Spectrally-overlapped chirped fibre Bragg grating sensor system for simultaneous two-parameter sensing" in *Meas. Sci. Technol.*, Vol. 18, No. 12, pp. 3825-3832 (2007).
- [25] H.Y. Fu, A.C.L. Wong, P.A. Childs, H.Y. Tam, Y.B. Liao, C. Lu, and P.K.A. Wai "Multiplexing of polarization-maintaining photonic crystal fiber based Sagnac interferometric sensors" in *Opt. Express*, Vol. 17, Iss. 21, pp. 18501-18512 (2009).
- [26] A.C.L. Wong, P. Childs, and G.D. Peng "Simultaneous demodulation technique for a multiplexed fibre Fizeau interferometer and a fibre Bragg grating sensor system" in *Opt. Lett.*, Vol. 31, No. 31, pp. 23-25 (2006).
- [27] A.C.L. Wong, P. Childs, and G.D. Peng "Multiplexed fibre Fizeau interferometer and fibre Bragg grating sensor system for simultaneous measurement of quasi-static strain and temperature using discrete wavelet transform" in *Meas. Sci. Technol.*, Vol. 17, No. 2, pp. 384-392 (2006).
- [28] Гельфанд И.М., Левитан Б.М. Об определении дифференциального уравнения по его спектральной функции // *Изв. АН СССР. Сер. мат.* 1951. Т. 15, № 4. С. 309-360 (in Russian).
- [29] Марченко В.А. Восстановление потенциальной энергии по фазам рассеянных волн // *Докл. АН СССР*. 1955. Т. 104, № 5. С. 695-698 (in Russian).
- [30] Захаров В.Е., Шабат А.Б. Точная теория двумерной самофокусировки и одномерной автомодуляции волн в нелинейных средах // *ЖЭТФ*. 1971. Т. 61, № 1. С. 118-134 (in Russian).
- [31] E.A. Robinson "Predictive decomposition of time series with application

- to seismic exploration” in *Geophysics*, Vol. 32, No. 3, pp. 418-484 (1967).
- [32] A.P. Goupillaud “An approach to inverse filtering of near-surface layer effects from seismic records” in *Geophysics*, Vol. 26, No. 6, pp. 754-760 (1961).
- [33] R. Feced, M.N. Zervas, and M.A. Muriel “An efficient inverse scattering algorithm for the design of nonuniform fiber Bragg gratings” in *IEEE J. Quantum Electron.*, Vol. 35, No. 8, pp. 1105-1115 (1999).
- [34] J. Skaar, L. Wang, and T. Erdogan “On the synthesis of fiber Bragg gratings by layer peeling” in *IEEE J. Quantum Electron.*, Vol. 37, No. 2, pp. 165-173 (2001).
- [35] J. Skaar, and R. Feced “Reconstruction of gratings from noisy reflection data” in *J. Opt. Soc. Am. A*, Vol. 19, Iss. 11, pp. 2229-2237 (2002).
- [36] A. Rosenthal, and M. Horowitz “Inverse scattering algorithm for reconstructing strongly reflecting fiber Bragg gratings” in *IEEE J. Quantum Electron.*, Vol. 39, No. 8, pp. 1018-1026 (2003).
- [37] L. Wang, and T. Erdogan “Layer peeling algorithm for reconstruction of long-period fibre gratings” in *Electron. Lett.*, Vol. 37, No. 3, pp. 154-156 (2001).
- [38] K. Kolossovski, A.V. Buryak, and R. Sammut “Optimised time-frequency domain layer-peeling algorithm to reconstruct fibre Bragg gratings” in *Electron. Lett.*, Vol. 40, No. 17, pp. 1046-1047 (2004).
- [39] O.V. Belai., E.V. Podivilov, O.Ya. Schwartz, and D.A. Shapiro “Finite Bragg grating synthesis by numerical solution of hermitian Gel'fand-Levitan-Marchenko equations” in *J. Opt. Soc. Am. B*, Vol. 23, Iss. 10, pp. 2040-2045 (2006).
- [40] O.V. Belai., L.L. Frumin, E.V. Podivilov, and D.A. Shapiro “Efficient numerical method of the fibre Bragg grating synthesis” in *J. Opt. Soc. Am. B*, Vol. 24, Iss. 7, pp. 1451-1457 (2007).
- [41] A.M. Bruckstein, I. Koltracht, and T. Kailath “Inverse scattering with noisy data” in *SIAM J. Sci. Statist. Comput.*, Vol. 7, Iss. 4, pp. 1331-1349 (1986).
- [42] A. Buryak, J. Bland-Hawthorn, and V. Steblina “Comparison of inverse scattering algorithms for designing ultrabroadband fibre Bragg gratings” in *Opt. Express*, Vol. 17, Iss. 3, pp. 1995-2004 (2009).
- [43] S. Huang, M. LeBlanc, M.M. Ohn, and R.M. Measures “Bragg intragrating structural sensing” in *Appl. Opt.*, Vol. 34, Iss. 22, pp. 5003-5009 (1995).
- [44] P. Childs, A.C.L. Wong, W. Terry, and G.D. Peng “Measurement of crack formation in concrete using embedded optical fibre sensors and differential strain analysis” in *Meas. Sci. Technol.*, Vol. 19, Iss. 6, (2008) paper 065301..
- [45] P.C. Won, J. Leng, Y. Lai, and J.A.R. Williams “Distributed temperature sensing using a chirped fibre Bragg grating” in *Meas. Sci. Technol.*, Vol. 15, Iss. 8, pp. 1501-1505 (2004).
- [46] Y. Okabe, R. Tsuji, and N. Takeda “Application of chirped fiber Bragg grating sensors for identification of crack locations in composites” in *Compos. A*, Vol. 35, Iss. 1, pp. 59-65 (2004).
- [47] A.M. Gillooly, K.E. Chisholm, L. Zhang and I. Bennion “Chirped fibre Bragg grating optical wear sensor” in *Meas. Sci. Technol.*, Vol. 15, Iss. 5, pp. 885-888 (2004).
- [48] J.A. Besley, L. Reekie, C. Weeks, T. Wang, and C. Murphy “Grating writing model for materials with nonlinear photosensitive response” in *J. Lightw. Technol.*, Vol. 21, Iss. 10, pp. 2421-2428 (2003).
- [49] G.M.H. Flockhart, G.A. Cranch, and C.K. Kirkendall “Rapid characterization of the ultraviolet induced fiber Bragg grating complex coupling coefficient as a function of irradiance and exposure time” in *Appl. Opt.*, Vol. 46, Iss. 34, pp. 8237-8243 (2007).
- [50] L. Poladian “Group-delay reconstruction for fiber Bragg gratings in reflection and transmission” in *Opt. Lett.*, Vol. 22, Iss. 20, pp. 1571-1573 (1997).
- [51] A. Rosenthal, and M. Horowitz “Reconstruction of long-period fiber gratings from their core-to-core transmission function” in *J. Opt. Soc. Am. A*, Vol. 23, No. 1, pp. 57-68 (2006).
- [52] J.E. Bridges, and R.A. Zalewski “Orthogonal detection to reduce common channel interference” in *Proc. IEEE*, Vol. 52, No. 9, pp. 1022-1028 (1964).
- [53] P. Childs “Multiplexed optical fibre sensor systems for civil engineering applications”, Ph.D. Thesis, University of New South Wales, 2007.
- [54] S.V. Miridonov, M.G. Shlyagin, and D. Tentori “Twin-grating fiber optic sensor demodulation” in *Opt. Commun.*, Vol. 191, Iss. 3-6, pp. 253-262 (2001).
- [55] P. Childs, and Y.B. Liao “On the multiplexed limit capacity of spectrally overlapped continuous wave FBG sensor networks” in *J. Opt.*, Vol. 12, Iss. 1, pp. 015404 (2010).
- [56] P. Childs, T. Whitbread, and G. D. Peng, “Spectrally coded multiplexing in a strain sensor system based on carrier-modulated fibre Bragg gratings” in *Proc. of SPIE*, Vol 5634, pp. 204-210 (2005).
- [57] B.H. Lee, and J. Nishii “Self-interference of long-period fibre grating and its application as a temperature sensor” in *Electron. Lett.*, Vol. 34, No. 21, pp. 2059-2060 (1998).
- [58] E.M. Dianov, S.A. Vasiliev, A.S. Kurkov, O.I. Medvedkov, and V.N. Protopopov “In-fiber Mach-Zehnder interferometer based on a pair of long-period gratings” in *Proc. ECOC*, Vol. 52, pp. 65-68 (1996).
- [59] P. Childs, A.C.L. Wong, I. Leung, G.D. Peng, and Y.B. Liao “An In-Line In-Fibre Ring Cavity Sensor for Localised Multi-Parameter Sensing” in *Meas. Sci. Technol.*, Vol. 19, No. 6, p. 065302 (2008).
- [60] X.J. Yu, P. Childs, M. Zhang, L.W. Wang, Y.B. Liao, J. Ju, and W. Jin “Relative humidity sensor based on cascaded long period gratings with hydrogel coatings” in *IEEE Photon. Technol. Lett.*, Vol 21, Iss 24, pp. 1828-1830 (2009).
- [61] I. Daubechies “The wavelet transform, time-frequency localization and signal analysis” in *IEEE Trans. Inform. Theory*, Vol. 36, No. 5, pp. 961-1005 (1990).
- [62] E.W. Aslaksen, and J.R. Klauder “Continuous representation theory using the affine group” in *J. Math. Physics*, Vol. 10, Iss. 12, pp. 2267-2275 (1969).
- [63] D. Estaban, and C. Galand “Application of quadrature mirror filters to split-band voice coding schemes” in *Proc. IEEE Intern. Conf. on Acoustics, Speech and Signal Processing*, Vol. 2, pp. 191-195 (1977).
- [64] M.J.T. Smith, and T.P. Barnwell III “A procedure for designing exact reconstruction filter banks for tree-structured subband coders” in *Proc. IEEE Intern. Conf. on Acoustics, Speech and Signal Processing*, Vol. 9, pp. 421-424 (1984).
- [65] Y. Meyer “Ondolettes et fonctions splines” in *Sem. Equations aux Derivees Partielles – Ecole Polytechnique*, Exp. 6, pp. 1-18, 1986-1987 (in French).
- [66] S.G. Mallat “A theory for multiresolution signal decomposition: The wavelet representation” in *IEEE Trans. Pattern Anal. Machine Intell.*, Vol. 11, No. 7, pp. 674-693 (1989)
- [67] S. Mann, and S. Haykin “The adaptive chirplet: an adaptive generalized wavelet-like transform” in *Proc. SPIE*, Vol. 1565, pp. 402-413 (1991).